University of HUDDERSFIELD

University of Huddersfield Repository

Muhamedsalih, Hussam, Jiang, Xiang and Gao, F.

Accelerated surface measurement using wavelength scanning interferometer with compensation of environmental noise

Original Citation

Muhamedsalih, Hussam, Jiang, Xiang and Gao, F. (2013) Accelerated surface measurement using wavelength scanning interferometer with compensation of environmental noise. Procedia Engineering: 12th CIRP Conference on Computer Aided Tolerancing, 10. pp. 70-76. ISSN 1877-7058

This version is available at https://eprints.hud.ac.uk/id/eprint/15357/

The University Repository is a digital collection of the research output of the University, available on Open Access. Copyright and Moral Rights for the items on this site are retained by the individual author and/or other copyright owners. Users may access full items free of charge; copies of full text items generally can be reproduced, displayed or performed and given to third parties in any format or medium for personal research or study, educational or not-for-profit purposes without prior permission or charge, provided:

- The authors, title and full bibliographic details is credited in any copy;
- A hyperlink and/or URL is included for the original metadata page; and
- The content is not changed in any way.

For more information, including our policy and submission procedure, please contact the Repository Team at: E.mailbox@hud.ac.uk.

http://eprints.hud.ac.uk/

Available online at www.sciencedirect.com

ScienceDirect

Procedia Engineering 00 (2011) 000–000

Procedia Engineering

www.elsevier.com/locate/procedia

12th CIRP Conference on Computer Aided Tolerancing

Accelerated surface measurement using wavelength scanning interferometer with compensation of environmental noise

H. Muhamedsalih*, X. Jiang and F. Gao

EPSRC Innovative Manufacure Reseach Centre in Advanced Metrology, Centre for Precision Technologies, School of Computing and Engineering, University of Huddersfield, Queensgate, Huddersfield, HD1 3DH, UK

Abstract

The optical interferometry has been widely explored for surface measurement due to the advantages of non-contact and high accuracy interrogation. Eventually, some interferometers are used to measure both rough and smooth surfaces such as white light interferometer and wavelength scanning interferometer (WSI). The WSI can measure large discontinuous surface profiles without the phase ambiguity problems. However, the WSI usually needs to capture hundreds of interferograms at different wavelength in order to evaluate the surface finish for a sample. Moreover, the measurement process might be affected by environmental disturbances if the surface inspection takes place in a production environment (e.g. in- process inspection). This paper introduces a wavelength scanning interferometer (WSI) for fast areal surface measurement of micro and nano-scale surfaces which is immune to environmental noise. The WSI system and operation principles are introduced in this paper. Mathematical description of data analysis is presented. This paper also describes an active servo control system that serves as a phase compensating mechanism to eliminate the effects of environmental noise. Finally, a parallel programming model is presented as a solution to accelerate the computing analysis in the WSI. This parallel programming is based on CUDATM C program structure that developed by NVIDIA. The presented system can be used for on-line or in-process measurement on the shop floor.

© 2011 Published by Elsevier Ltd. Selection and/or peer-review under responsibility of CIRP CAT 2012

Keywords: wavelength scanning interferometry; parallel programming; surface measurement

1. Introduction

Optical interferometers are widely used in metrology for surface inspection because of the non-contact measurement methodology, high measurement resolution and high throughput inspection. Various interferometry methods of surface inspection have been developed for different applications such as phase shift interferometry, white light interferometry and wavelength scanning interferometer. The phase shift interferometry is typically used for measurements that require high resolution and throughput. The main

*Coresponding author. Tel:+44-1484-472983; fax: +44-1484-472161
Email: h.muhamedsalih@hud.ac.uk

limitation of this type of interferometry is the phase ambiguity that occurs when measuring discontinuous surfaces with heights exceed a half of the illumination wavelength [1]. This limitation was overcome by developing a white light interferometry. Measuring the coherence of white light is used to indicate the zero optical path difference position (i.e OPD=0) for each measurement point [2]. Typically, the coherence measurement is evaluated by performing mechanical scanning using a piezo-electric transducer. The WSI interferometer is used to measure large discontinuous surfaces without any mechanical scanning. This kind of interferometer was reported by many researchers worldwide in the field of areal surface measurement such as Kuwamura and Yamaguchi [3].

In this paper, the wavelength scanning process is achieved by using an acousto optical tunable filter (AOTF). The phase and surface measurement principle is described. A servo control technique is used to stabilize the interferometer during the measurement process. The measurement results on the semiconductor daughterboard under mechanical disturbance show the system can withstand environmental noise. This paper also describes a parallel programming method to accelerate the computing process in order to increase the inspection throughput. A CUDA C program is proposed to achieve data parallelism for accelerating a computing analysis of the captured data. The presented measurement system can be used in on-line or in-process measurement to measure and characterize freeform structured surfaces.

2. The WSI System

The interferometry system, shown in figure 1, is composed of a Linnik interferometer, a halogen white light source and acousto-optic tunable filter (AOTF). The AOTF is a key feature of this experimental setup. It is placed after a halogen white light to diffract a specific wavelength and pass to a Linnik interferometer. The wavelength diffraction depends on the AOTF driving frequency. Thus by changing the driving frequency, wavelength scanning process is achieved. In this experiment, the wavelength is scanned from 682.8nm to 552.8nm with less than 1.5nm bandwidth resolution at each wavelength.

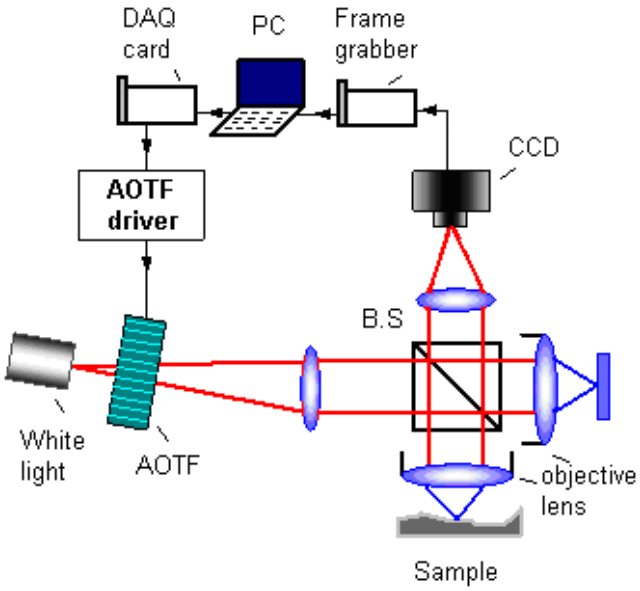

Fig. 1. WSI configuration

During wavelength scanning process, 128 frames are captured by the CCD hence each frame is captured at a specific wavelength. Every pixel in a captured frame represents a specific point upon the surface of a measured sample. Therefore, the intensity values captured by each CCD pixel are gathered and analyzed individually. Since the optical path difference is fixed at each pixel, a sinusoidal intensity distribution is obtained from the wavelength scanning process as shown in figure 2.a. Each point in this distribution has it own scanned wavelength. Equation 1 describes the mathematical expression of the intensity distribution.

$$I_{xy}(i) = a_{xy} + b_{xy}\cos(\phi_{xy}(i)) \tag{1}$$

I is an intensity value captured by a CCD pixel. i is the iteration of the captured frame number (1,2,..,FN). x and y are the pixel numbers in horizontal and vertical directions of the CCD respectively. a and b are constant values. These constant values are function of the light intensities that reflect from interferometer arms. φ is the phase shift caused by altering wavelength of the broadband light. The phase of the intensity distribution depends on the scanned wavelength and the optical path difference (i.e. height of the measured sample), as described in equation 2.

$$\phi(i) = \frac{2\pi}{\lambda_i} * 2h \tag{2}$$

λ_i is the scanning wavelength and h is the sample step height. Fourier transform algorithm (FFT) is used to manipulate the captured intensity pattern and determine the surface structure.

The captured frames obtained from WSI, are evaluated by using FFT method of fringe pattern analysis [4]. The intensity values of each pixel need to be gathered and analyzed individually from other pixels. This section describes a mathematical approach to evaluate the data captured by one of the CCD pixels. The mathematical expression of equation 1 can be rewritten in form of equation 3 for the convenience of explanation.

$$I_{xy}(i) = a_{xy}(i) + \frac{1}{2}b_{xy}\, e^{j\phi_{xy}(i)} - \frac{1}{2}b_{xy}\, e^{-j\phi_{xy}(i)} \tag{3}$$

Equation 3 can be simplified by considering the following notations

$$c = \frac{1}{2}b\,e^{j\phi} \text{ and } c^* = \frac{1}{2}b\,e^{-j\phi}$$

$$I_{xy}(i) = a + c + c^* \tag{4}$$

FFT is applied to equation 4 to find the spectrum of the intensity distribution. The spectrum contains three main terms as stated in equation 5. The first term is constant amplitude that related to the light intensity in each interferometer arm, the second and third terms are related to the phase change of a fringe which recorded by a CCD pixel.

The purpose of FFT is to distinguish between the useful information which is induced by the phase change (i.e. c or c^* term) and the unwanted information of constant amplitude (i.e. A). The spectrum of equation 5 can be rewritten in a matrices form as shown in equation 6. The f_o is a spatial frequency corresponded to the wavelength scanning and it is function of the optical path difference.

$$FFT[I(i)] = A(f) + C(f - f_o) + C^*(f + f_o) \tag{5}$$

$$FFT\begin{pmatrix} I(1) \\ I(2) \\ . \\ . \\ . \\ . \\ I(n) \end{pmatrix}_{xy} = \begin{pmatrix} A(f) \\ . \\ C(f-f_o) \\ . \\ . \\ C^*(f+f_o) \\ . \end{pmatrix}_{xy} \tag{6}$$

The unwanted spectrum A and C^* are filtered out by replace their values to zeros as shown matrix 7. The inverse FFT is applied to matrix 7 to reconstruct the c value in equation 4.

$$Filteration\ result = \begin{pmatrix} 0 \\ . \\ C(f-f_o) \\ 0 \\ . \\ 0 \\ 0 \end{pmatrix}_{xy} \tag{7}$$

Then, natural logarithm is applied to separate the phase φ from the unwanted amplitude variation b, as illustrated in equation 8 and 9.

$$I' = ln[\frac{1}{2} b\, e^{j\phi}] = ln[\frac{1}{2} b] + j\phi \tag{8}$$

$$\begin{pmatrix} I'(1) \\ I'(2) \\ . \\ . \\ . \\ . \\ I'(n) \end{pmatrix}_{xy} = ln(ifft\begin{pmatrix} 0 \\ . \\ C(f-f_o) \\ . \\ 0 \\ 0 \\ 0 \end{pmatrix}_{xy}) = \begin{pmatrix} ln(0.5b(1) \mp j\varphi(1)) \\ ln(0.5b(2) \mp j\varphi(2)) \\ . \\ . \\ . \\ . \\ ln(0.5b(n) \mp j\varphi(n)) \end{pmatrix}_{xy} \tag{9}$$

Each determined values in equation 9 consists of real and imaginary parts. The phase shifts are extracted from the imaginary parts as shown in Figure 2.b. This figure suffers from discontinuities because the computed phase is limited with range of $-\pi$ to π. These discontinuities are corrected by adding 2π to the discontinuous parts in order to obtain a continuous phase distribution as shown figure 2.c.

Finally, the optical path difference (*OPD*) is determined from the slop of the phase as stated in equation 10.

$$OPD = \frac{\Delta\phi}{2\pi\left[\frac{1}{\lambda_m} - \frac{1}{\lambda_n}\right]} \tag{10}$$

$\Delta\varphi$ is the change in phase between any two points in figure 4. λm and λn are the correspondence wavelengths of phase difference ($\Delta\varphi$).

In order to obtain the areal topography for the captured sample, the described analysis steps should be applied to the entire pixels. As example, to find the areal topography of a sample viewed by 640x480 CCD pixels, the data analysis needs to be executed 307200 times in a sequential manner if a tradition C program is used with multicore CPUs. This evaluation strategy can significantly reduce the measurement throughput. Therefore, a parallel programming model is proposed to accelerate the computing process using GTX280 GPUs as explained in section 4.

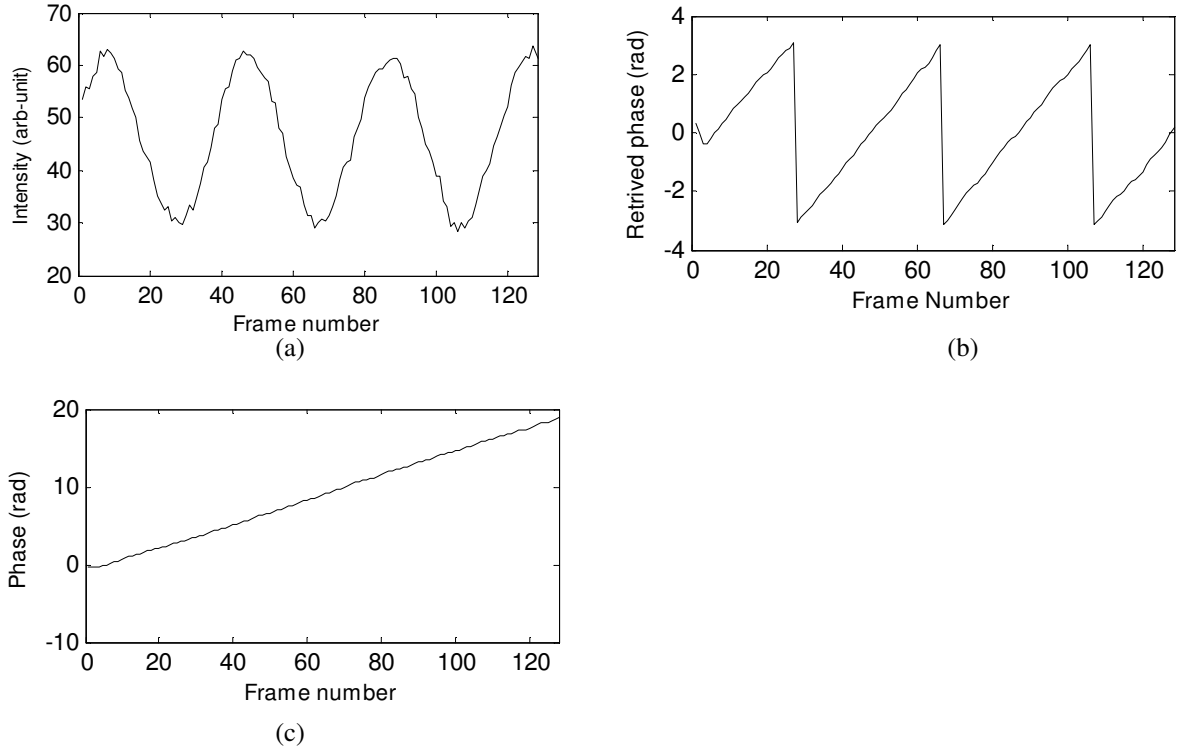

Fig. 2. Measured Interference fringe and retrived phase distribution (a) intensity distribution of 128 frames for one pixel (b) retrived phase discontinuity distribution (c) phase continuity distribution.

3. Vibration Compensation

The optical configuration that introduced in figure 1 is modified by adding a second interferometer known as a reference interferometer. The WSI and reference interferometer are multiplexed and shared a

common optical path as shown in figure 3. The light source of the reference interferometer is a Super Luminescent Light Emitting Diode (SLED)) and operates at 830nm wavelength. Thus, the two interferometers shared the same environmental disturbances. The WSI interferometer is used to measure the surface structure as described in section 2 and the reference interferometer is used as a feedback source for a close loop control system in order to stabilise the entire interferometry. The two beams paths of the interferometers are combined by a Dichroic mirror DM1 to induce a common beams path and transferred into a Linnik interferometer. The output beams path of the Linnik interferometer are separated by Dichroic mirror DM2. The WSI interferometer output is detected by two dimensional CCD arrays, while the reference interferometer output is detected by Silicon PIN detector. The output of the detector is fed into a PI controller which controls a piezo transducer (PI.840-10) movement to compensate for vertical mechanical vibration. The piezo transducer is attached to the reference mirror. Thus, the reference mirror can trace a disturbance mechanical vibration of the sample and keep the optical path difference fixed.

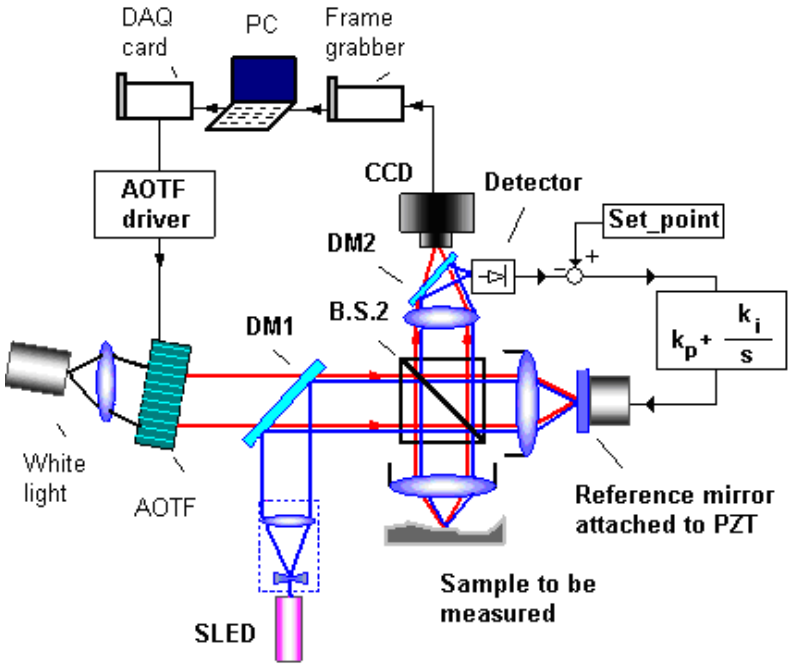

Fig. 3. Stabilised WSI interferometer

4. Results of the Stabilised WSI

The effectiveness of the vibration compensation has been investigated by carrying out the following experiments. In the first part of the experiment, a semiconductor daughterboard sample is measured without inducing a mechanical disturbance as shown in Figure 4(a). One profile of the sample is shown in Figure 4(b) and illustrates the surface step with height 5.22 µm.

In the second part of the experiment, a sinusoidal mechanical disturbance of 40 Hz and 400 nm peak to peak is applied to the sample using a PZT. During the disturbance, the sample is measured (Figure 5).

Figure 5(a) shows that the measured signals are suppressed by the mechanical vibration signal. One of the sample profile, figure 5(b), shows that the surface roughness signal is completely distorted.

When the vibration compensation is switched on, a reduction in the disturbance movement of the fringe pattern is clearly observed. The measurement of the sample at this stage is carried out (Figure 6). Figure 6(a) shows that the data has been retrieved again as the original measurement and illustrates that the compensation vibration can be used to overcome environmental disturbance. One profile of the sample cross-section plot in figure 6(b) shows the step height is 5.20 µm. The difference of the two measured step height value is 13.5 nm in comparing the two measured results as shown in Figure 4(b) and Figure 6(b).

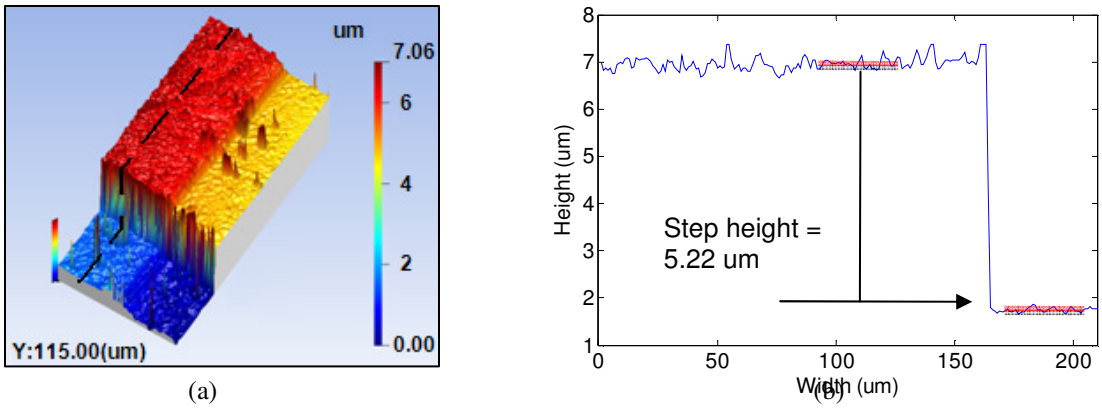

(a) (b)

Fig. 4. Measurement result of semiconductor daughterboard sample without an induced mechanical disturbance. (a) measured surface and (b) cross-sectional profile.

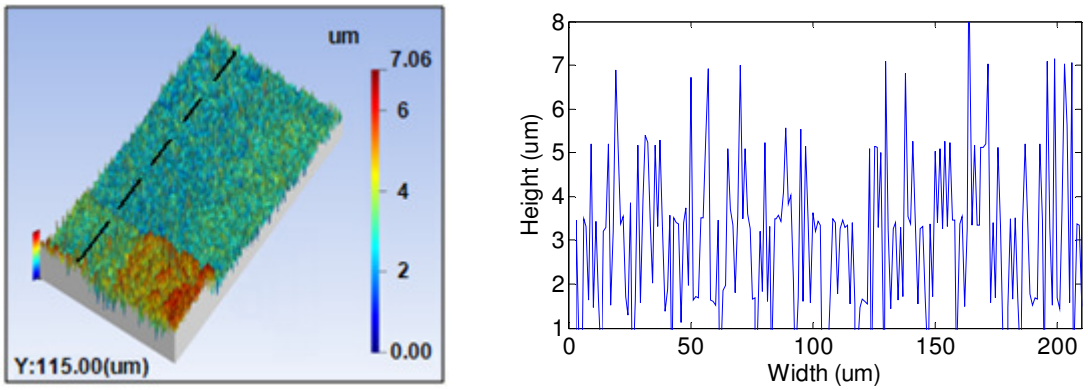

(a) (b)

Fig. 5. Measurement result of semiconductor daughterboard sample with a sinusoidal mechanical disturbance of 40 Hz and 400nm peak to peak. (a) measured surface and (b) cross-sectional profile.

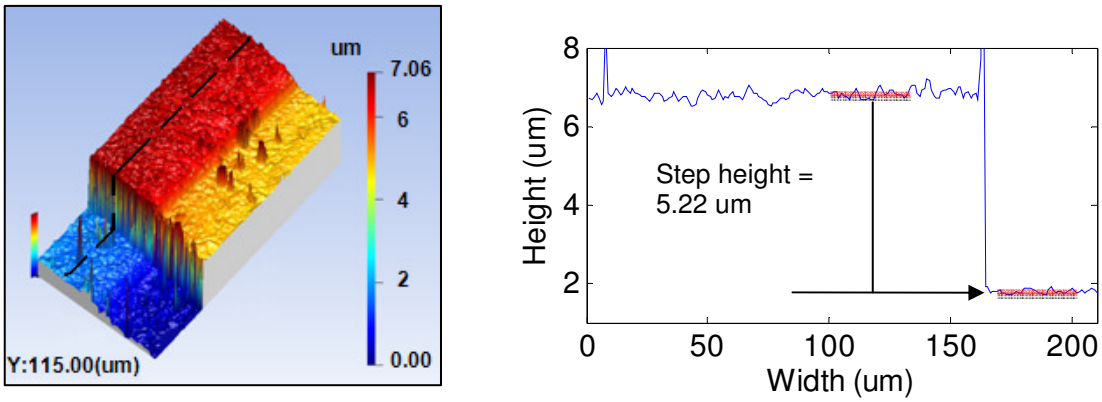

(a) (b)

Fig. 6. Measurement result of semiconductor daughterboard sample with vibration compensation. (a) measured surface and (b) cross-sectional profile.

5. Acceleration of Computing Process

The evaluating process for areal topography needs long processing time if CPUs traditional sequential execution programs are used. The CUDA C program is used to achieve the data parallelism using a GPU device, hence increasing the measurement throughput. Typically, in a sequential programming model, the program generates a main thread that executes functions in a sequential manner. In contrast, the CUDA parallel programming model generates thousands to millions number of thread to execute data-parallel functions, know as kernels, in a parallel manner [5].

The demonstrated WSI measurement in figures 4 is based on capturing 128 frames during the wavelength scanning process. The captured frames are stored in the CPU main memory in a successive manner (i.e. frame by frame). The form of the captured data is re-arranged into pixel by pixel form. Thus, each pixel can be analyzed individually. Then, the new form of data is transferred to the GPU memory using API CUDA memory arrangement functions. The GPU can accommodate thousands to millions generated threads to analysis the data. In the proposed program structure, the generated threads are equal to number of captured pixels. Hence, each pixel data is evaluated through a specific thread. For example, the demonstrated measurement in figure 4 is captured by 640x480 pixels. Thus, 307200 threads are generated to analyze the data. The flow chart of the proposed program is illustrated in figure 7. This flow chart is mainly constructed from four written kernels and two FFT functions. The written kernels are data filtration, phase determination, phase correction and optical path difference determination. The two, FFT and inverse FFT, functions are part of NVIDIA CUFFT library [6].

The accelerated result of the proposed program is shown in table 1. This table shows the effectiveness of the parallel programming performance for the proposed system. The measurement of figure 4 was repeated four times with different frame rates (i.e. 64, 128, 256 and 512 respectively). The captured frames size is (640x480) pixels. The computing time using GeForce GTX 280, were compared to those obtained from sequential execution Matlab simulation, using Intel® Core™2 Duo CPU. Nevertheless, the acceleration factor is reduced when the captured frame number is increased. This is typically because of the memory limitation of the GTX 285 according to the proposed measurement method. The reduction in

the acceleration factor can be enhanced by using up-to-date GPUs which are continuously improved in terms of the number of processing cores and the size of memory spaces.

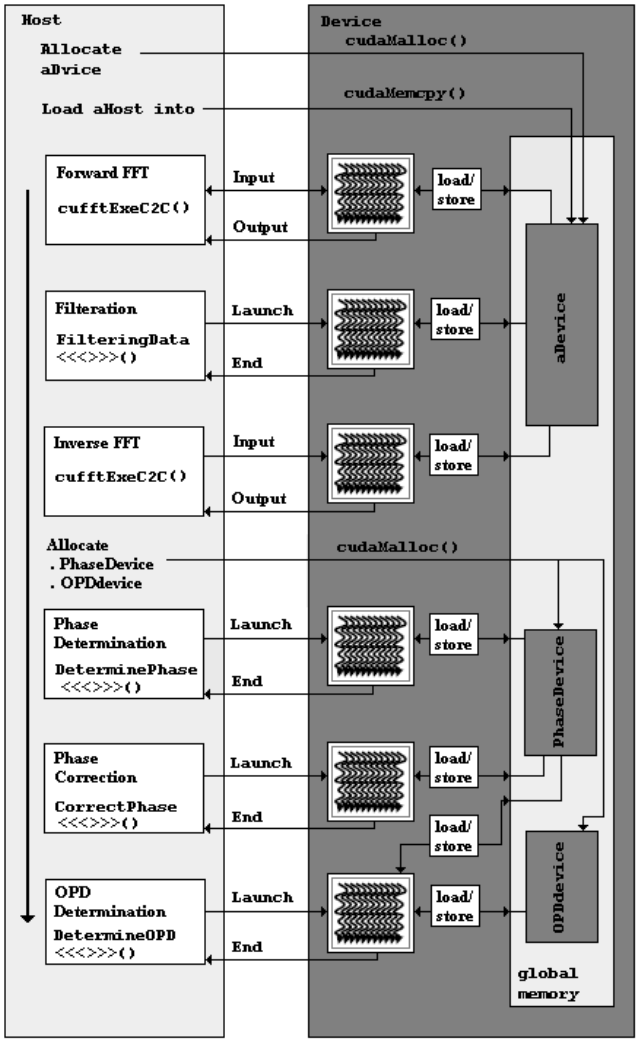

Fig. 7. The proposed CUDA program structure.

Table 1 Parallel programming performance versus sequential programming.

Frame Number	64	128	256	512
Matlab Processing Time (sec)	12.03	20.711	31.99	61.22
CUDA C Processing time (sec)	0.18	0.42	1.16	2.84
Accelerating Factor	66.1	49.1	27.6	21.5

6. Conclusion

We have proposed a surface measurement technique with active control of environmental noise that utilizes wavelength scanning interferometry. The WSI is used for areal measurements of discontinues profiles surfaces without phase ambiguity. The AOTF provides a fast wavelength scanning technique to produce phase shift information. The produced phase shift is evaluated by the FFT. An 830nm wavelength SLED sharing the same optical path of the measurement interferometer can be used to introduce a feedback loop for vibration compensation. The measurement throughput for the proposed WSI system can be improved by using parallel programming on GPUs. The proposed CUDA C parallel programming is used with GPU type GTX285 to accelerate the computing process up to 49 times approximately for 128 captured frames.

Acknowledgement

The authors gratefully acknowledge the Engineering and Physical Sciences Research Council (EPSRC) UK for supporting this research work under its IKC programme. The author X. Jiang gratefully acknowledges the Royal Society under a Wolfson-Royal Society Research Merit Award and the European Research Council under its programme ERC-2008-AdG 228117-Surfund.

References

[1] Caber, P. "Interferometric profiler for rough surfaces." Applied Optics 32(19): (1993) 3438-3441.

[2] Schwider, J. and L. Zhou. "Dispersive interferometric profilometer." Optics Letters 19(13): (1994) 995.

[3] Kuwamura, S. and I. Yamaguchi. "Wavelength scanning profilometry for real-time surface shape measurement." OSA Optical Society of America 36(19): (1997) 4473

[4] Takeda, M., I. Hideki, et al.. "Fourier-transform method of fringe-pattern analysis for computer-based topography and interferometry." OSA Optical Society of America 72(1): (1982) 156-160.

[5] NVIDIA. (2008). " NVIDIA CUDA Compute Unified Device Architecture: programming guide 2.0." from http://developer.download.nvidia.com/compute/cuda/2_0/docs/NVIDIA_CUDA_Programming_Guide_2.0.pdf.

[6] NVIDIA. (2007). "CUDA CUFFT Library." Retrieved 20 May, 2011, from http://moss.csc.ncsu.edu/~mueller/cluster/nvidia/0.8/NVIDIA_CUFFT_Library_0.8.pdf.